3D Object Recognition Based on Canonical Angles between Shape Subspaces

Yosuke Igarashi and Kazuhiro Fukui

Graduate School of Systems and Information Engineering,
University of Tsukuba, Japan
igarashi@cvlab.cs.tsukuba.ac.jp, kfukui@cs.tsukuba.ac.jp

Abstract. We propose a method to measure similarity of shape for 3D objects using 3-dimensional shape subspaces produced by the factorization method. We establish an index of shape similarity by measuring the geometrical relation between two shape subspaces using canonical angles. The proposed similarity measure is invariant to camera rotation and object motion, since the shape subspace is invariant to these changes under affine projection. However, to obtain a meaningful similarity measure, we must solve the difficult problem that the shape subspace changes depending on the ordering of the feature points used for the factorization. To avoid this ambiguity, and to ensure that feature points are matched between two objects, we introduce a method for sorting the order of feature points by comparing the orthogonal projection matrices of two shape subspaces. The validity of the proposed method has been demonstrated through evaluation experiments with synthetic feature points and actual face images.

1 Introduction

In this paper, we propose a method to measure the similarity of 3D object shapes based on the geometrical relation between shape subspaces produced by the factorization method [1]. Using the proposed shape similarity measure, we realize 3D object recognition that is invariant to camera rotation and object motion.

The factorization method [1] is one of the most successful geometry-based methods for recovering the 3D shape of an object. The factorization method tracks the positions of multiple feature points through an image sequence and constructs a measurement matrix $\mathbf{W}$, which contains the 2D positions of the tracked feature points. The measurement matrix $\mathbf{W}$ is then factored into the product of a motion matrix $\mathbf{U}$ and a shape matrix $\mathbf{V}$. The motion matrix represents the camera rotation and the shape matrix represents the 3D positions of the object in a coordinate system attached to the object center.

The columns of the shape matrix span a 3-dimensional subspace, which is called the *shape subspace*. Shape subspace is invariant, under affine projection, to changes of coordinates caused by camera rotation and object motions [2, 3]. Therefore, the concept of shape subspace has been used in various tasks, such

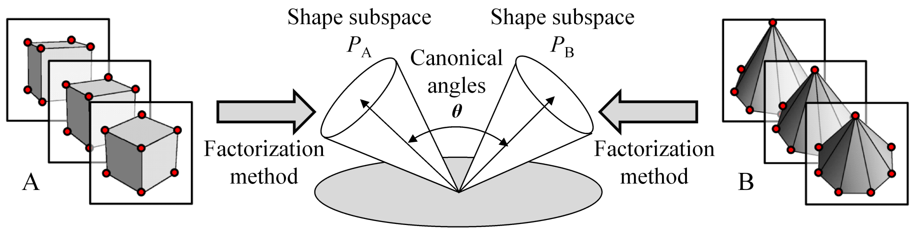

Fig. 1. Proposed framework of 3D object recognition based on canonical angles between shape subspaces.

as motion segmentation [4–6] and sequential factorization [7]. This useful characteristic of shape subspaces leads us the idea that a shape similarity that is invariant to camera rotation and object motion can be established by measuring the geometrical relation between two shape subspaces. The shape subspace includes information about geometrical relations among multiple feature points. Therefore, we can obtain an index of the structural similarity between two sets of multiple feature points by measuring the canonical angles [8] between the two shape subspaces.

The usefulness of canonical angles (also called principal angles) has recently been established in applications in the field of computer vision, such as face recognition [9], where the relation between two subspaces representing distributions of face patterns is determined. Canonical angles have also been used for the motion segmentation of a non-ridge object [10], such as the human body. In this application, canonical angles are used to find the dimension of the intersection of two motion spaces that are produced by the factorization method. The dimension of the intersection indicates whether two parts are linked by a point or an axis.

Figure 1 shows the proposed framework for 3D object recognition. First, the feature points are tracked through image sequence for each object, and then the shape subspaces of the two objects are derived from the sets of the tracked feature points by the factorization method. Finally, the canonical angles between the shape subspaces are found and used to construct a measure of shape similarity. To obtain a robust measure of the similarity between shape subspaces, we have to overcome the problem that shape subspaces change depending on the order of the feature points used to construct a measurement matrix.

To do this, we use the concept of an orthogonal projection matrix, which is uniquely determined from the orthogonal basis vectors of a shape subspace. The core of our idea is to minimize the difference between the two orthogonal projection matrices, which are generated from the feature points of two objects, by rearranging the rows and the columns of one of them. The feature points are taken to have been matched between two objects when the difference between the two matrices is the smallest.

Several methods have been proposed for matching feature points based on shape subspaces. Wang and Xiao [11] applied QR factorization to the orthogonal projection matrices, and then permuted the rows in matrix $\mathbf{Q}$ to produce a correspondence between shape subspaces. Marques and Costeira [12] used linear programming to compute a transformation matrix for minimizing the difference between the orthogonal projection matrices. In this paper, we will compare the performance of the QR-based method with that of the proposed method, since both methods involve permuting a matrix.

The rest of the paper is organized as follows. Section 2 briefly describes the characteristics of shape subspaces. In Section 3, we propose the method for matching two sets of feature points and measuring shape similarity. In Section 4, we demonstrate the validity of the proposed method through experiments with a synthetic 3D object and images of real faces. Section 5 contains our conclusions.

2 Calculation procedure of shape subspace

In this section, we outline how a shape subspace is generated. There are two calculation procedures: one is based on the factorization [1] of an image sequence, and the other is based on the positions of multiple feature points on an object.

2.1 Factorization of an image sequence

The factorization method [1] can robustly recover the shape and motion of an object from an image sequence without assuming a model of motion, such as constant translation or rotation. An image sequence can be represented as a $2F \times P$ measurement matrix $\mathbf{W}$, with P points tracked through F frames as follows:

$$\mathbf{W} = \begin{pmatrix} x_{11} & \dots & x_{1P} \\ y_{11} & \cdots & y_{1P} \\ \vdots & \ddots & \vdots \\ x_{F1} & \dots & x_{FP} \\ y_{F1} & \cdots & y_{FP} \end{pmatrix}, \tag{1}$$

where x_{fp} and y_{fp} are the 2D coordinates of the pth point in frame f.

If image coordinates are given with respect to their centroids, the measurement matrix $\mathbf{W}$ is factored into the product of three matrices:

$$\mathbf{W} = \mathbf{U}\mathbf{\Sigma}\mathbf{V}^T \simeq \mathbf{U}'\mathbf{\Sigma}'\mathbf{V}'^T, \tag{2}$$

where $\mathbf{U}$ is a $2F \times 2F$ orthogonal matrix and $\mathbf{V}$ is a $P \times P$ orthogonal matrix. $\mathbf{\Sigma}$ is a $2F \times P$ diagonal matrix with the singular values σ_i of $\mathbf{W}$ in descending order. Here, the rank of matrix $\mathbf{W}$ is 3 due to the geometrical constraint, so $\sigma_4, ..., \sigma_D = 0$ (or are very small). Hence, $\mathbf{W}$ can be represented as the product of a $2F \times 3$ matrix $\mathbf{U}'$, a 3×3 diagonal matrix Σ' and a $3 \times P$ matrix $\mathbf{V}'^T$ as shown in Eq. (2).

The column vectors of the *shape matrix* $\mathbf{V}'$ span the *shape subspace*. The shape subspace is invariant under an affine transformation of the set of feature points [4], such as that caused by camera rotation or object motion.

2.2 Generation based on the coordinates of multiple points

If the 3D coordinates of all the multiple feature points of an object are known, the shape subspace can be obtained directly without using the factorization method.

The shape subspace corresponding to an object is spanned by the column vectors of the $P \times 3$ matrix $\mathbf{S}$ defined by

$$\mathbf{S} = (\boldsymbol{r}_1 \ \boldsymbol{r}_2 \ \ldots \ \boldsymbol{r}_P)^T = \begin{pmatrix} x_1 & y_1 & z_1 \\ \vdots & \vdots & \vdots \\ x_P & y_P & z_P \end{pmatrix}, \tag{3}$$

where $\boldsymbol{r}_p = (x_p \ y_p \ z_p)^T$ for $1 \leq p \leq P$ denotes the positional vector of the pth point on an object. These vectors satisfy the relation $\sum_{p=1}^{P} \boldsymbol{r}_p = \mathbf{0}$. In this definition, the shape subspace is invariant to the selection of coordinates.

3 The proposed method

In this section, we first propose a method for matching feature points using an orthogonal projection matrix. Then, we explain how to measure the geometrical similarity between two shape subspaces using the canonical angles [8].

3.1 Matching feature points using orthogonal projection matrices

The shape subspace is the column space of $\mathbf{V}'$ in Eq. (2) or of $\mathbf{S}$ in Eq. (3). If the orders of feature points change, the shape subspace corresponding to them also changes. Therefore, we need to match the feature points between two objects to obtain shape similarity based on the geometric relation between shape subspaces.

The key property of the orthogonal projection matrix The proposed method is based on the fact that an orthogonal projection matrix is uniquely determined by its corresponding object.

Let $\boldsymbol{\Phi} = (\boldsymbol{\phi}_1 \ \boldsymbol{\phi}_2 \ \ldots \ \boldsymbol{\phi}_M)$ be an orthonormal basis for the M-dimensional subspace $\mathcal{P}$. The orthogonal projection matrix $\mathbf{P}$ is then defined by

$$\mathbf{P} = \sum_{i=1}^{M} \boldsymbol{\phi}_i {\boldsymbol{\phi}_i}^T = \boldsymbol{\Phi}\boldsymbol{\Phi}^T. \tag{4}$$

Two shape matrices $\mathbf{V}_A$ and $\mathbf{V}_B$ obtained from the same object are not always equal, even if their feature points correspond to each other, because each shape matrix is just one set of basis vectors of the shape subspaces. Therefore, we cannot use the shape matrices to match the feature points. However, the two orthogonal projection matrices calculated from $\mathbf{V}_A$ and $\mathbf{V}_B$ using Eq. (4) always coincide:

$$\mathbf{Q} = \mathbf{V}_A \mathbf{V}_A^T = \mathbf{V}_B \mathbf{V}_B^T. \tag{5}$$

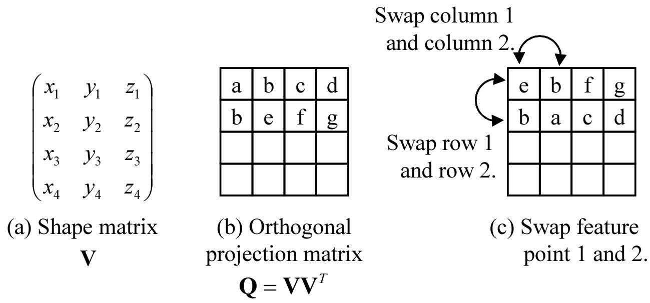

Fig. 2. Example of swapping rows and columns of the orthogonal projection matrix by swapping feature points. ($P = 4$)

Based on this property, we match of feature points by rearranging the rows and columns of the orthogonal projection matrices corresponding to both objects, instead of handling the shape matrices.

Exchanging feature points Exchanging the order of two feature points on an object is equivalent to permuting the rows and columns of the orthogonal projection matrix. We will illustrate how to exchange the order of feature points by considering the following simple case.

Suppose that four feature points are extracted from an object. Figures 2 (a) and (b) show the shape matrix $\mathbf{V}$ and the orthogonal projection matrix $\mathbf{Q}$ calculated from $\mathbf{V}$. If feature point 1 and feature point 2 are exchanged, then the 1st row and the 2nd row are swapped in $\mathbf{Q}$, and the 1st column and the 2nd column are also exchanged at the same time, as shown in Fig. 2 (c). Note that the sets of the elements of the 1st row of (b) and the 2nd row of (c) are the same, although the orders of the elements are different. This rule is obeyed even if the number of the feature points to be exchanged increases.

Based on this rule, we can compare the rows of the orthogonal projection matrices by sorting the elements of the rows of each projection matrix in advance. The problem of matching feature points then reduces to finding the pairs of row vectors closest each other.

The matching algorithm The procedure is as follows:
INPUT: $N \times N$ Orthogonal projection matrices $\mathbf{X}_A$ and $\mathbf{X}_B$ generated from N feature points of two objects A and B
OUTPUT: $N \times 2$ Correspondence matrix $\mathbf{C}$

1. **Initialization**: $\mathbf{Q}_{A(0)} = \mathbf{X}_A$, $\mathbf{Q}_{B(0)} = \mathbf{X}_B$
2. **for** $t = 0$ to N **do**
   (a) Sort the unmasked elements of $\mathbf{Q}_{A(t)}$ and $\mathbf{Q}_{B(t)}$ within each row to produce temporary matrices $\mathbf{Q}'_{A(t)}$ and $\mathbf{Q}'_{B(t)}$.

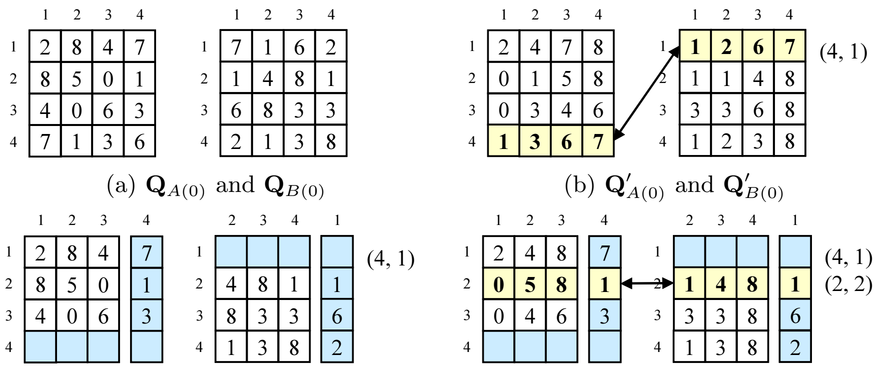

(a) $\mathbf{Q}_{A(0)}$ and $\mathbf{Q}_{B(0)}$ (b) $\mathbf{Q}'_{A(0)}$ and $\mathbf{Q}'_{B(0)}$

(c) $\mathbf{Q}_{A(1)}$ and $\mathbf{Q}_{B(1)}$ (d) $\mathbf{Q}'_{A(1)}$ and $\mathbf{Q}'_{B(1)}$

Fig. 3. Example of the proposed matching process. In this example, these matrices are not orthogonal projection matrices, although they are symmetric matrices. (a) shows the input matrices $\mathbf{Q}_{A(0)}$ and $\mathbf{Q}_{B(0)}$. In (b), the matrices are sorted within each row to produce temporary matrices $\mathbf{Q}'_{A(0)}$ and $\mathbf{Q}'_{B(0)}$. The 4th row of $\mathbf{Q}'_{A(0)}$ and the 1st row of $\mathbf{Q}'_{B(0)}$ are matched, as their L_1-norm is the smallest. In (c), the 4th row of $\mathbf{Q}_{A(0)}$ and the 1st row of $\mathbf{Q}_{B(0)}$ are masked from the lists to be matched. Then, the 4th column and the 1st column are paired. These matrices are defined as $\mathbf{Q}_{A(1)}$ and $\mathbf{Q}_{B(1)}$. In (d), the non-corresponding elements of the rows of $\mathbf{Q}_{A(1)}$ and $\mathbf{Q}_{B(1)}$ are sorted. These matrices are $\mathbf{Q}'_{A(1)}$ and $\mathbf{Q}'_{B(1)}$. Then, the 2nd row of $\mathbf{Q}'_{A(1)}$ and the 2nd row of $\mathbf{Q}'_{B(1)}$ are matched.

(b) Find a pair of rows of $\mathbf{Q}'_{A(t)}$ and $\mathbf{Q}'_{B(t)}$ with the minimum L_1-norm distance. The distance function between the row vectors, $\boldsymbol{u}_i$ of $\mathbf{Q}'_{A(t)}$ and $\boldsymbol{v}_j$ of $\mathbf{Q}'_{B(t)}$, is defined as follows:
$$d(\boldsymbol{u}_i, \boldsymbol{v}_j) = \sum_{k=1}^{N} |u_{ik} - v_{jk}| \quad (t = 0) ,$$
$$d(\boldsymbol{u}_i, \boldsymbol{v}_j) = \sum_{k=1}^{N-t} |u_{ik} - v_{jk}| + \sum_{k=1}^{t} |x^*_{ki} - y^*_{kj}| \quad (t \geq 1) .$$
The row numbers found in the searcing, r_A and r_B, are set to the tth row vector $\boldsymbol{c}_t$ of $\mathbf{C}$, as $\boldsymbol{c}_t = (r_A, r_B)$.

(c) Mask the r_Ath row and the r_Ath column $\boldsymbol{x}^*_{(t+1)}$ of $\mathbf{Q}_{A(t)}$, and the r_Bth row and the r_Bth column $\boldsymbol{y}^*_{(t+1)}$ of $\mathbf{Q}_{B(t)}$, respectively. These masked matrices are set to $\mathbf{Q}_{A(t+1)}$ and $\mathbf{Q}_{B(t+1)}$.

3. **end for**

Figure 3 shows a simple example of this matching procedure.

3.2 Similarity between shape subspaces

First, we introduce canonical angles; then, we define the similarity between shape subspaces using them.

Consider an M-dimensional subspace $\mathcal{S}_A$ and an N-dimensional subspace $\mathcal{S}_B$, where $M \leq N$. Given $\boldsymbol{u}_i \in \mathcal{S}_A$ and $\boldsymbol{v}_i \in \mathcal{S}_B$, the canonical angles θ_i

$(\theta_1 \leq \theta_2 \leq \ldots \leq \theta_M)$ are uniquely defined by [8]

$$\cos^2\theta_i = \sup_{\substack{\boldsymbol{u}_i \perp \boldsymbol{u}_j,\ \boldsymbol{v}_i \perp \boldsymbol{v}_j \\ 1 \leq i,j \leq M,\ i \neq j}} \frac{(\boldsymbol{u}_i \cdot \boldsymbol{v}_i)^2}{||\boldsymbol{u}_i||^2 ||\boldsymbol{v}_i||^2}, \tag{6}$$

where $(\cdot)$ denotes the inner product and $||\cdot||$ denotes the norm of a vector.

Let $\mathbf{Q}_A$ and $\mathbf{Q}_B$ denote the orthogonal projection matrices of the subspaces $\mathcal{S}_A$ and $\mathcal{S}_B$. Then, $cos^2\theta$ for the canonical angle θ between $\mathcal{S}_A$ and $\mathcal{S}_B$ is equal to the eigenvalue of $\mathbf{Q}_A\mathbf{Q}_B$ or $\mathbf{Q}_B\mathbf{Q}_A$ [8]. The largest eigenvalue corresponds to the smallest canonical angle θ_1, whereas the second largest eigenvalue corresponds to the smallest angle θ_2 in a direction perpendicular to that of θ_1. The values of $cos^2\theta_i$ ($i = 3, \ldots, M$, and $M \leq N$) are calculated similarly.

From these canonical angles, we define the shape similarity φ by

$$\varphi = \frac{1}{M}\sum_{i=1}^{M} cos^2\theta_i. \tag{7}$$

If two shape subspaces coincide completely with each other, φ is 1.0, since all canonical angles are zero. The similarity φ gets smaller as the two spaces separate. Finally, the similarity φ is zero when the two subspaces are orthogonal to each other.

3.3 3D object recognition based on the proposed similarity measure

Figure 4 shows the proposed procedure, from inputting the image sequences of two objects A and B to the output of the shape similarity index.

First, multiple feature points are tracked through an image sequence of object A by a tracker, such as the Kanade-Lucas-Tomasi (KLT) feature tracker [13]. Then, the measurement matrix $\mathbf{W}_A$ is calculated from the positions of the tracked feature points. Next, the measurement matrix $\mathbf{W}_A$ is factored into the product of the shape matrix $\mathbf{V}_A$ and the motion matrix $\mathbf{U}_A$. A shape matrix $\mathbf{V}_B$ and a motion matrix $\mathbf{U}_B$ are also obtained from the image sequence for object B. The orthogonal projection matrices $\mathbf{Q}_A$ and $\mathbf{Q}_B$ are calculated from $\mathbf{V}_A$ and $\mathbf{V}_B$. Their rows and columns are rearranged to match feature points. Then, the shape similarity φ can be calculated from the shape subspaces using Eq. (7).

4 Experimental results

In this section, we first use synthetic data to evaluate the accuracy of the proposed algorithm for matching feature points, and then use images of real faces to demonstrate the effectiveness of the proposed method for object recognition.

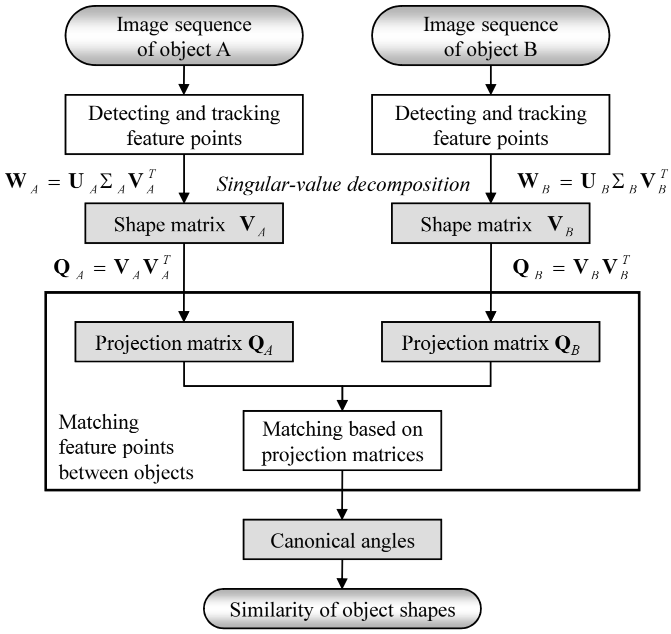

Fig. 4. Flow of the object recognition process based on the proposed similarity measure.

4.1 Experiment I: Matching feature points using synthetic data

We evaluate the robustness of the proposed matching method using a synthetic 3-dimensional data set. We prepared two sets of feature points for the evaluation experiment. The first set is a set of P randomly generated points on an unit sphere. The second set is the first set with added Gaussian noise of standard deviation σ. Two shape matrices were generated from both the sets of feature points using Eq. (3) in Sec. 2.2. We compared the proposed matching method with the matching method based on QR factorization [11] described in Sec. 1.

Figure 5 shows an example of feature-point matching for $P = 30$ and $\sigma = 0.1$. Figure 6 shows a comparison of the error rates of the two methods of matching for various values of the parameters P and σ. For each of the parameters, 200 independent experiments were run. The proposed method consistently shows a lower error rate than the QR based method [11]. When $\sigma = 0.1$ and $P = 30$, the error rate is about 20% (see Fig. 6 (a)). If $P = 100$ and $\sigma = 0.0316$, the error rate with our method is about 5% (see Fig. 6 (b)). We conclude that the proposed matching method has high accuracy and is robust even under high noise conditions.

4.2 Experiment II: Face recognition

We now consider the application of the proposed method to face recognition. The surface of a human face has many feature points, such as moles and freckles,

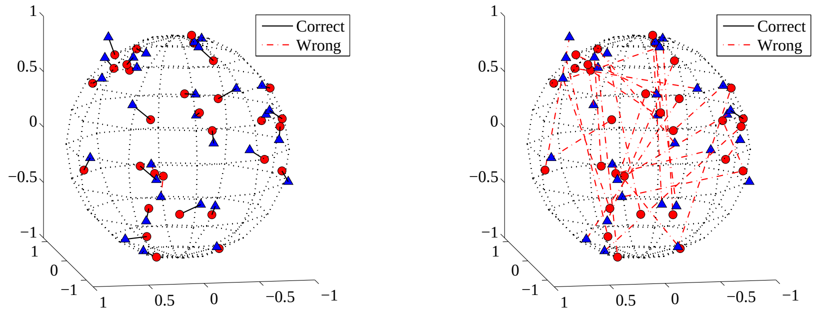

(a) Proposed method (b) QR based method [11]

Fig. 5. Example of matched feature points on spheres ($P = 30, \sigma = 0.1$).

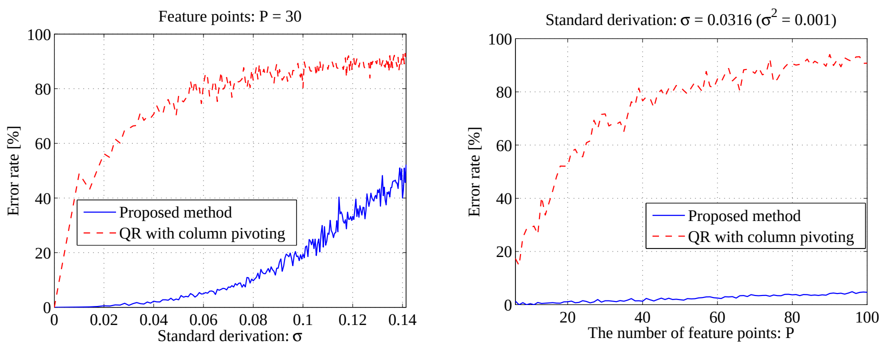

(a) (b)

Fig. 6. Performances of the proposed matching method: (a) error rate vs. level of noise ($P = 30$) and (b) error rate vs. the number of feature points ($\sigma = 0.0316$).

which are distinct characteristics that can be used to identify individuals. The effectiveness of using these feature points for face recognition has been shown by Pierrard and Vetter [14]. We detected moles and freckles from facial images using a circular separability filter [15], and used them as feature points.

The number of participants was 22. A participant sat on a chair about 1 meter away from a camera. We captured 300 frames for each participant, while the head was moving. The image size was 1024×768 pixels.

Figure 7 shows examples of the input image, detected face region and separability map. First, we detected the facial region [16] and the regions of pupils and nostrils [15]; we then remove the latter regions from the facial region, because they are common features of all subjects. Next, we applied a circular separability filter to obtain a separability map. Finally, we detected and tracked 26 feature

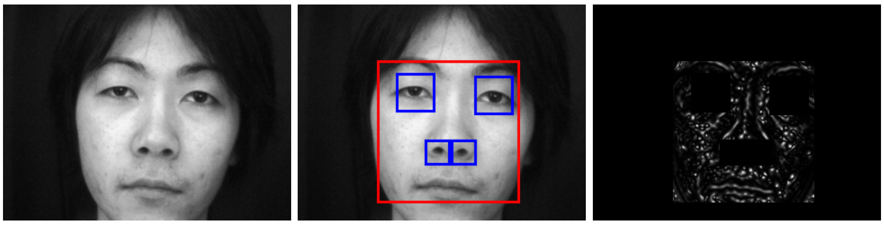

(a) (b) (c)

Fig. 7. Pre-processing for generating the shape subspace: (a) input image, (b) detected face, pupils and nostrils, (c) separability map.

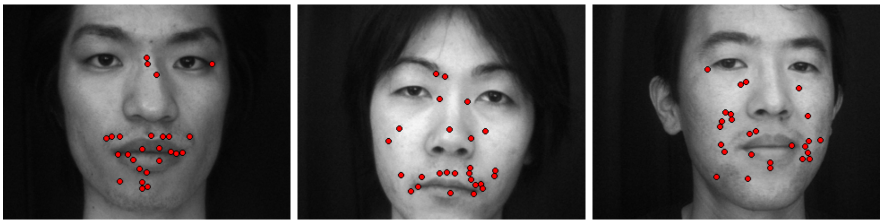

Fig. 8. Examples of detected and tracked feature points ($P = 26$).

points from the 300 separability maps by applying the KLT feature tracker [13]. Figure 8 shows examples of the tracked feature points.

The 300 frames were divided into sets of 30 frames for each of the 22 subjects so that we obtained 220 datasets. A shape subspace was generated from each dataset by the factorization method. We compared the proposed matching method and the conventional matching method using QR factorization in terms of classification performance. The input subspace generated from a set of input image sequences was classified using the Nearest Neighbor algorithm. The classification rate was estimated by the Leave-One-Out method.

Figure 9 shows an example of the feature points matched. Figure 10 shows the similarity maps among the sets of sequential images by the proposed method. Figure 10 (a) shows the result by the proposed matching method and (b) shows that by the conventional method. Table 1 lists the recognition rates and Equal Error Rate (EER), which is defined as the crossing point of the False Acceptance Rate and False Rejection Rate curves. The value of ERR should be as low as possible to achieve high performance face recognition.

From Table 1 we can see that the proposed matching method is superior to the conventional, QR-based method. The recognition rate of the proposed method was 99.5% with 22 subjects whereas the recognition rate using the QR-based method was 94.1%. The large difference between the performances of the two methods seems to derive from the degree of robustness of feature extraction against ambiguity resulting from added noise and occlusions. Moreover, the EER

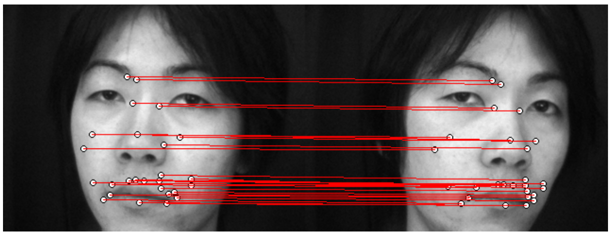

Fig. 9. An example of feature points matched between two image sequences.

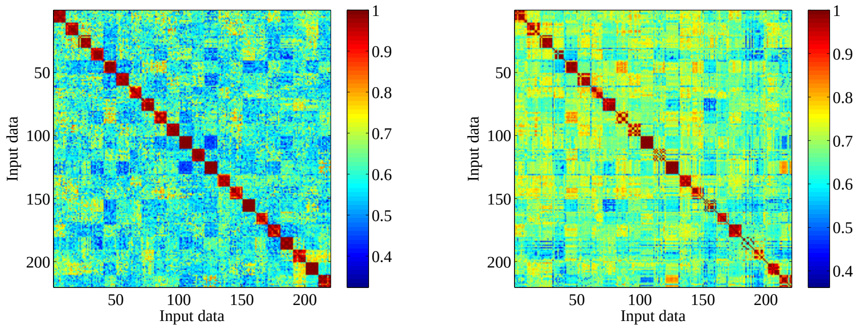

(a) (b)

Fig. 10. Similarity maps based on the canonical angles for face recognition with 22 subjects: (a) using the proposed matching method and (b) using the conventional method based on QR factorization [11].

of the proposed method is very low: it is only 2.60%, compared to 17.3% for the QR-based method. These results clearly support the validity of our framework for 3D object recognition based on the canonical angles between shape subspaces.

5 Conclusions

In this paper, we have proposed a method for measuring the similarity between 3D object shapes, which is invariant to camera rotation and object motion. The proposed measure of shape similarity is based on the shape subspaces produced by the factorization method. The shape subspace produced depends on the order

Table 1. Comparison between the proposed method and the conventional method for face recognition.

Matching method	Recognition rate	EER
Proposed	99.5%(219/220)	2.60%
QR-based [11]	94.1%(207/220)	17.30%

of the feature points considered. To avoid this ambiguity, we have proposed a method of matching the feature points of two objects by rearranging the rows and columns of their orthogonal projection matrices.

We have confirmed through an evaluation experiment using synthetic data that the proposed matching method can match the feature points of two objects. Our method is more robust to noise than the conventional method based on QR factorization. We have also demonstrated that a framework based on the combination of shape similarity and our matching method is effective for classifying facial images.

References

1. Tomasi, C., Kanade, T.: Shape and motion from image streams under orthography: a factorization method. International Journal of Computer Vision **9** (1992) 137–154
2. Poelman, C.J., Kanade, T.: A paraperspective factorization method for shape and motion recovery. Pattern Analysis and Machine Intelligence **19** (1997) 206–218
3. Begelfor, E., Werman, M.: Affine invariance revisited. Computer Vision and Pattern Recognition **2** (2006) 2087–2094
4. Costeira, J.P., Kanade, T.: A multi-body factorization method for independently moving objects. International Journal of Computer Vision **29** (1998) 159–179
5. Ichimura, N.: Motion segmentation based on factorization method and discriminant criterion. International Conference on Computer Vision **1** (1999) 600–605
6. Kanatani, K.: Motion segmentation by subspace separation and model selection. International Conference on Computer Vision **2** (2001) 586–591
7. Morita, T., Kanade, T.: A sequential factorization method for recovering shape and motion from image streams. Pattern Analysis and Machine Intelligence **19** (1997) 856–867
8. Chatelin, F.: Eigenvalues of Matrices. John Wiley & Sons (1993)
9. Fukui, K., Yamaguchi, O.: Face recognition using multi-viewpoint patterns for robot vision. International Symposium of Robotics Research (2003) 192–201
10. Yan, J., Pollefeys, M.: A factorization-based approach for articulated nonrigid shape, motion and kinematic chain recovery from video. Pattern Analysis and Machine Intelligence **30** (2008) 867–877
11. Wang, Z., Xiao, H.: Dimension-free affine shape matching through subspace invariance. Computer Vision and Pattern Recognition (2009) 2482–2487
12. Marques, M., Costeira, J.: Lamp: Linear approach for matching points. International Conference on Image Processing (2009) 2113–2116
13. Tomasi, C., Kanade, T.: Detection and tracking of point features. Carnegie Mellon University Technical Report **CMU-CS-91-132** (1991)
14. Pierrard, J.S., Vetter, T.: Skin detail analysis for face recognition. Computer Vision and Pattern Recognition (2007) 1–8
15. Fukui, K., Yamaguchi, O.: Facial feature point extraction method based on combination of shape extraction and pattern matching. Systems and Computers in Japan **29** (1998) 49–58
16. Viola, P., Jones, M.: Rapid object detection using a boosted cascade of simple features. Computer Vision and Pattern Recognition (2001) 511–518